NEW DIFFRACTION DATA

Crystal structure of Form 2 of racemic reboxetine mesylate, (C$_{19}$H$_{24}$NO$_3$)(CH$_3$O$_3$S)

James Kaduk[1,2] ⓘ, Anja Dosen[3] ⓘ and Tom Blanton[3] ⓘ

[1]*Department of Chemistry, Illinois Institute of Technology, 3101 South Dearborn Street, Chicago, IL 60616, USA*
[2]*Department of Physics, North Central College, 131 South Loomis Street, Naperville, IL 60540, USA*
[3]*International Centre for Diffraction Data (ICDD), 12 Campus Boulevard, Newtown Square, PA 19073-3273, USA*

Abstract: The crystal structure of a new form of racemic reboxetine mesylate has been solved and refined using synchrotron X-ray powder diffraction data and optimized using density functional theory techniques. Reboxetine mesylate crystallizes in space group $P2_1/c$ (#14) with $a = 14.3054(8)$, $b = 18.0341(4)$, $c = 16.7924(11)$ Å, $\beta = 113.4470(17)°$, $V = 3{,}974.47(19)$ Å^3, and $Z = 8$ at 298 K. The crystal structure consists of double columns of anions and cations along the a-axis. Strong N–H···O hydrogen bonds link the cations and anions into zig-zag chains along the a-axis. The powder pattern has been submitted to the International Centre for Diffraction Data (ICDD®) for inclusion in the Powder Diffraction File™ (PDF®). © The Author(s), 2025. Published by Cambridge University Press on behalf of International Centre for Diffraction Data. This is an Open Access article, distributed under the terms of the Creative Commons Attribution licence (http://creativecommons.org/licenses/by/4.0), which permits unrestricted re-use, distribution and reproduction, provided the original article is properly cited. [doi:10.1017/S0885715625100973]

Key words: reboxetine, Edronax®, crystal structure, Rietveld refinement, density functional theory

I. INTRODUCTION

Reboxetine, as the mesylate salt (sold under the brand name Edronax®), is an antidepressant used to treat clinical depression, panic disorder, and Attention Deficit Disorder (ADD)/attention Deficit Hyperactivity Disorder (ADHD). The systematic name (CAS Registry No. 98769-84-7) is (2R)-2-[(R)-(2-ethoxyphenoxy)-phenylmethyl]morpholinium methanesulfonate. A two-dimensional molecular diagram of reboxetine mesylate is shown in Figure 1.

X-ray powder diffraction data for the fumarate and succinate salts of reboxetine are reported in European Patent EP 1515959A1 (Zampieri et al., 2003; Pfizer Italia SRL). Powder data for several crystalline forms of reboxetine hydrochloride are reported in US Patent Application US 2010/0069389 A1 (Kalofonos et al., 2010; Bionevia Pharmaceuticals, Inc.). A crystal structure of what we designate Form 1 of racemic reboxetine mesylate was determined by MicroED in space group $P2_1/c$ with $a = 20.00$, $b = 5.49$, $c = 19.06$ Å, and $\beta = 107.338°$ (Lin et al., 2024). The structure was deposited with the Cambridge Crystallographic Data Centre as entry 2323516.

This work was carried out as part of a project (Kaduk et al., 2014) to determine the crystal structures of large-volume commercial pharmaceuticals and include high-quality powder diffraction data for them in the Powder Diffraction File (Kabekkodu et al., 2024).

II. EXPERIMENTAL

Reboxetine mesylate was a commercial reagent, purchased from TargetMol (Batch #T6963), and used as received. The white powder was packed into a 0.5-mm-diameter Kapton capillary and rotated during the measurement at ~2 Hz. The powder pattern was measured at 298(1) K at the Wiggler Low Energy Beamline (Leontowich et al., 2021) of the Brockhouse X-ray Diffraction and Scattering Sector of the Canadian Light Source using a wavelength of 0.819826(2) Å (15.1 keV) from 1.6 to 75.0° 2θ with a step size of 0.0025° and a collection time of 3 minutes. The high-resolution powder diffraction data were collected using eight Dectris Mythen2 X series 1 K linear strip detectors. NIST SRM 660b LaB$_6$ was used to calibrate the instrument and refine the monochromatic wavelength used in the experiment.

The pattern was difficult to index. Using the rule of thumb of 18 Å^3 per non-H atom, we expect a unit cell volume of an integral multiple of 504 Å^3. Several indexing programs yielded larger unit cells, with volumes from 2,500 to 2,900 Å^3, resulting in unreasonable Z-values and/or voids in the crystal structure. Once we became aware of the Lin et al. structure, those (minor) Form 1 peaks were removed from the peak list. The successful indexing was obtained by JADE Pro (MDI, 2024), excluding the Lin et al. peaks and those with $I_{rel} < 1\%$. Up to three unindexed peaks were permitted. The suggested cell had $a = 14.31682$, $b = 18.01376$, $c = 16.84149$ Å, $\beta = 113.54°$, $V = 3{,}981.92$ Å^3, and $Z = 8$. The suggested space group was $P2_1/c$, which was confirmed by the successful solution and refinement of the structure and confirmed that our sample was also racemic.

The reboxetine cation and mesylate anion molecular structures were extracted from the Lin et al. (2024) structure and saved

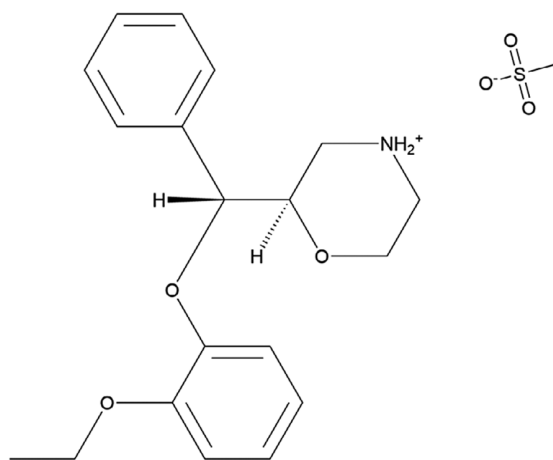Corresponding author: James Kaduk; Email: kaduk@polycrystallography.com

Figure 1. The two-dimensional structure of reboxetine mesylate.

as separate .mol2 files using Mercury (Macrae et al., 2020). The structure was solved using Monte Carlo-simulated annealing techniques as implemented in EXPO2014 (Altomare et al., 2013). Two cations and two anions were used as fragments, and a bump penalty was applied. One of the 10 solutions was significantly better than the others.

In the best solution, the protonated N4 in the morpholine ring of molecule 1 (lower atom numbers) formed the expected N–H⋯O hydrogen bonds to two anions, but the equivalent N51 in molecule 2 did not. The examination of the structure showed that C54 was 2.867 and 2.951 Å from two O atoms of the anions and, thus, was probably a nitrogen atom. The atom types in the morpholine ring were reassigned manually, and the hydrogen positions were recalculated using Mercury (conceptually rotating the ring by 180°) to obtain the model for refinement.

Rietveld refinement was carried out with GSAS-II (Toby and Von Dreele, 2013). Only the 2.5–55.0° portion of the pattern was included in the refinements (d_{min} = 0.888 Å). All non-H-bond distances and angles were subjected to restraints, based on a Mercury/Mogul Geometry Check (Bruno et al., 2004; Sykes et al., 2011). The Mogul average and standard deviation for each quantity were used as the restraint parameters. The aromatic rings in the cations were restrained to be planar. The restraints contributed 4.2% to the overall χ^2. The hydrogen atoms were included in calculated positions, which were recalculated during the refinement using Materials Studio (Dassault Systèmes, 2024). The U_{iso} of the heavy atoms were grouped by chemical similarity. Some U_{iso} refined to slightly negative values; therefore, they were fixed at reasonable values. The peak profiles were described using the generalized (Stephens, 1999) microstrain model. The background was modeled using a six-term-shifted Chebyshev polynomial, with peaks at 3.02 and 10.48° to model the narrow and broad scattering from the Kapton capillary and any amorphous component of the sample.

The final refinement of 203 variables using 21,201 observations and 138 restraints yielded the residual R_{wp} = 0.09959. The largest peak (0.27 Å from O48) and hole (1.47 Å from O96) in the difference Fourier map were 0.53(11) and −0.46 (11) $e\text{Å}^{-3}$, respectively. The final Rietveld plot is shown in Figure 2. The largest features in the normalized error plot are at three unindexed peaks at d-spacings = 5.3810, 4.4953, and 4.2997 Å, and in the shapes and positions of some of the strong low-angle peaks. The refined concentration of the Lin et al. phase was 5.1 wt%. The unindexed peaks indicate that the sample contains at least one additional crystalline phase, and the analyzed specimen has probably changed by the X-ray exposure during the measurement.

The crystal structure of reboxetine mesylate was optimized (fixed experimental unit cell) with density functional theory techniques using VASP (Kresse and Furthmüller, 1996) through the MedeA graphical interface (Materials Design, 2024). The calculation was carried out on 32 cores
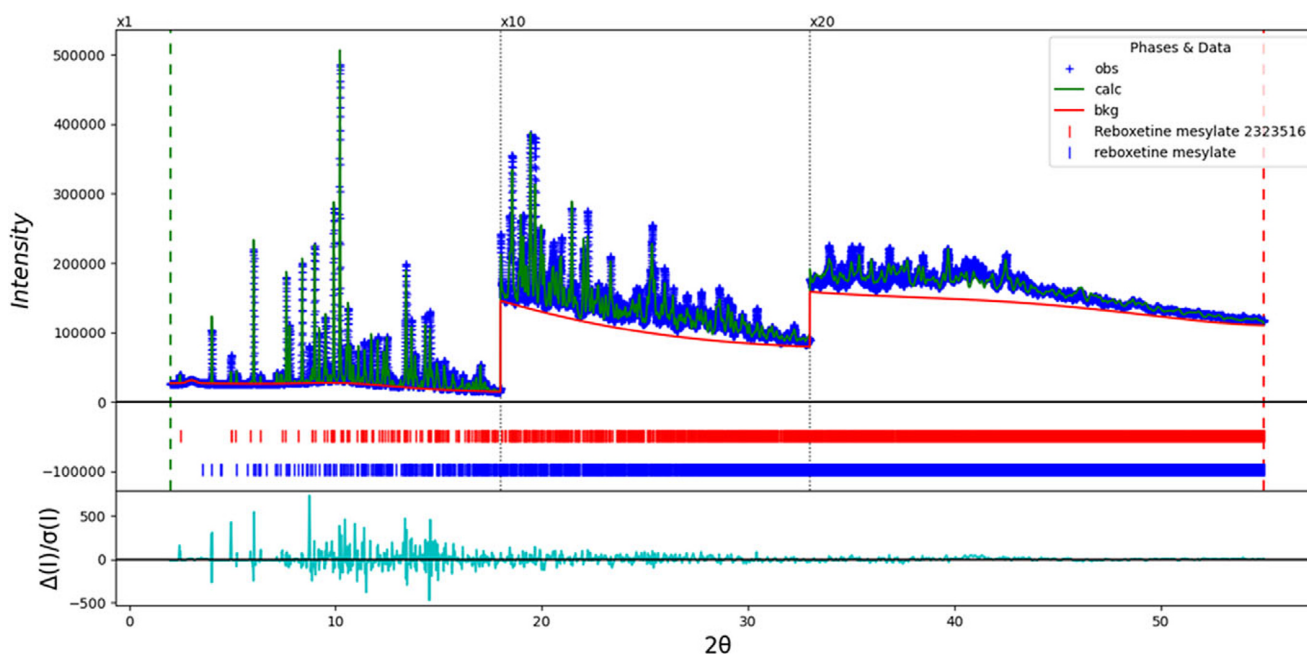

Figure 2. The Rietveld plot for reboxetine mesylate Form 2. The blue crosses represent the observed data points, and the green line represents the calculated pattern. The cyan curve indicates the normalized error plot, and the red line indicates the background curve. The blue tick marks indicate the Form 2 peak positions, and the red tick marks are for Form 1. The vertical scale has been multiplied by a factor of 10× for 2θ > 18.0° and by a factor of 20× for 2θ > 33.0°.

of a 144-core (768-GB memory) HPE Superdome Flex 280 Linux server at North Central College. The calculation used the GGA-PBE functional, a plane wave cutoff energy of 400.0 eV, and a k-point spacing of 0.5 Å^{-1}, leading to a $1 \times 1 \times 1$ mesh, and took ~22 hours. The crystal structure of Form 1 was optimized using the same strategy, except that a DFT-D3 dispersion correction was applied, and the lattice parameters were refined. Single-point density functional calculations (fixed experimental cell) and population analyses were carried out using CRYSTAL23 (Erba et al., 2023). The basis sets for the H, C, N, and O atoms in the calculation were those of Gatti et al. (1994), and the basis set for the S atom was that of Peintinger et al. (2013). The calculations were run on a 3.5-GHz PC using eight k-points and the B3LYP functional and took ~12.1 and 2.4 hours for Form 1 and Form 2, respectively.

III. RESULTS AND DISCUSSION

The sample of reboxetine mesylate studied here is a mixture (Figure 3). It contains 5.1 wt% of the previously characterized form, which we designate Form 1. The new Form 2 is the major phase, and a small concentration of at least one other crystalline phase is present. The thermal expansion of Form 1 is anisotropic (Table I), being greatest in the c-direction.

The structure of Form 1 reported by Lin et al. (2024) does not contain the expected N–H⋯O hydrogen bonds between the cation and the anion. However, C1 (using their atom numbering) was 2.821 and 2.960 Å from two of the O atoms in the sulfonate, indicating that it was probably a N. Using Materials Studio, O7 was changed to a C, C3 to O, C1 to N, and N2 to C, and the attached hydrogens recalculated, effectively rotating the morpholine ring by 180°. The atom numbering was changed by the program. Both the as-reported and this modified structure were optimized using VASP, including a dispersion correction and

TABLE I. Lattice parameters (space group $P2_1/c$) of reboxetine mesylate Form 1

Source	Lin et al.	This work	Ratio 298/80	DFT-D
T, K	80	298		
a, Å	20.000(4)	20.051(5)	1.0025	19.37736
b, Å	5.490(2)	5.5203(4)	1.0055	5.27407
c, Å	19.060(4)	19.308(4)	1.0130	18.50783
β, °	107.34(3)	108.628(11)		106.3993
V, Å^3	1,997.7(10)	2,025.19(23)	1.0138	1,814.501

TABLE II. Lattice parameters (space group $P2_1/c$) of reboxetine mesylate Form 2

Source	This work	DFT-D	Δ, %
a, Å	14.3054(8)	13.63088	−4.7
b, Å	18.0341(4)	17.58936	−2.5
c, Å	16.7924(11)	16.28194	−3.0
β, °	113.4470(17)	112.2081	−1.1
V, Å^3	3,974.47(19)	3,614.141	−9.1

allowing the cell to vary. The modified structure is 23.1 kcal/mol lower in energy; therefore, the modified structure is the basis for the remaining discussion. The modified Form 1 is 0.6 kcal/mol lower in energy than Form 2, but the difference is within the expected uncertainty of such calculations. It is unclear which form is more stable. For each form, the VASP-optimized lattice parameters are about 3% smaller than the observed ones (Tables I and II).

The root-mean-square (rms) difference of the non-H atoms in the Rietveld-refined and VASP-optimized structures of reboxetine mesylate Form 2, calculated using the Mercury CSD-Materials/Search/Crystal Packing Similarity tool, is 0.295 Å (Figure 4). The rms Cartesian displacements of the non-H atoms in the optimized structures of cation 1 and
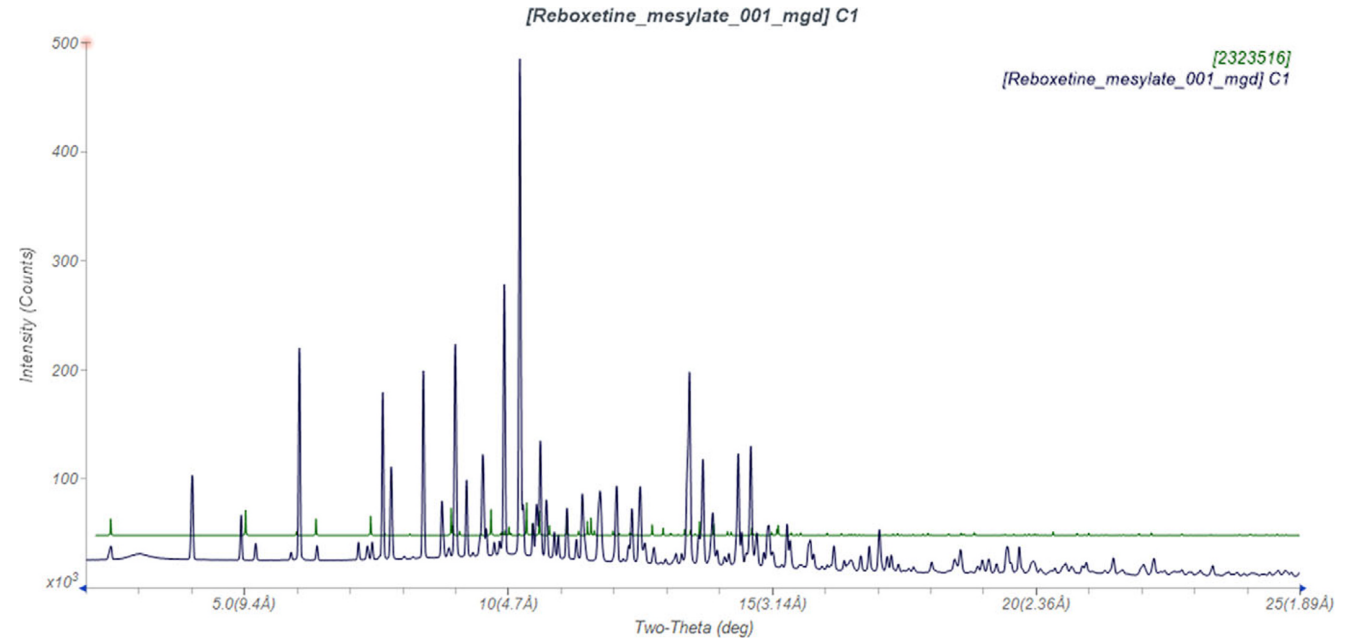

Figure 3. The synchrotron pattern from this study of reboxetine mesylate Form 2 (black), with the pattern calculated from the 80 K structure of Form 1 (Lin et al., 2024; green). Image generated using JADE Pro (MDI, 2024).
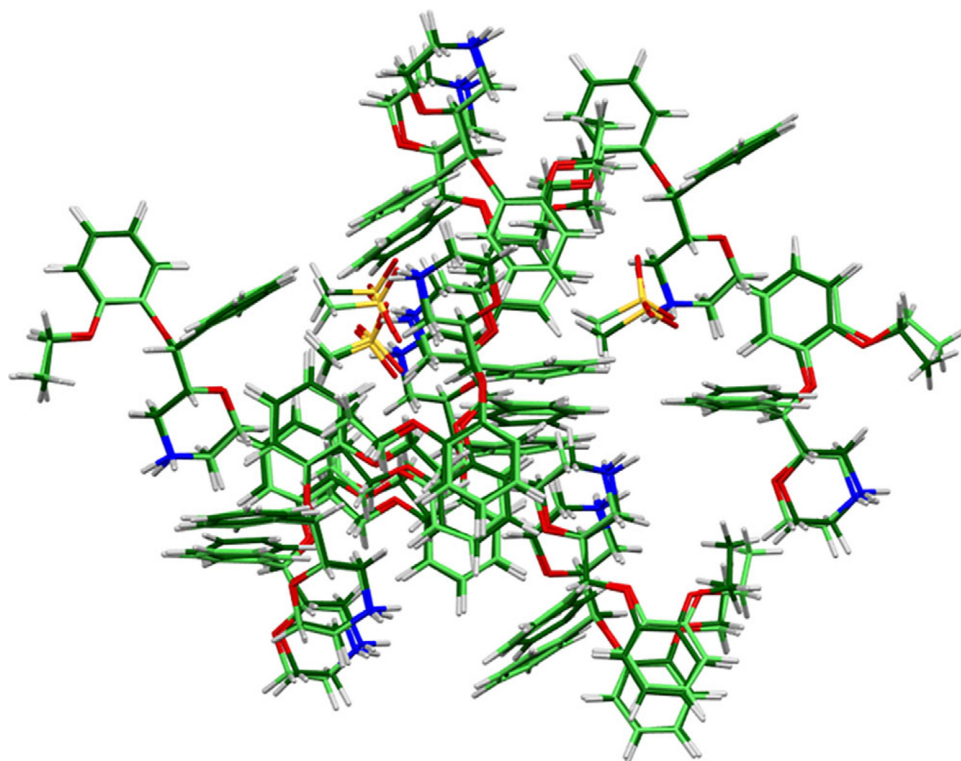
Figure 4. Comparison of the refined structure of reboxetine mesylate Form 2 (colored by atom type) to the VASP-optimized structure (light green). The comparison was generated by the Mercury CSD-Materials/Search/Crystal Packing Similarity tool; the rms displacement is 0.295 Å. Image generated using Mercury (Macrae et al., 2020).
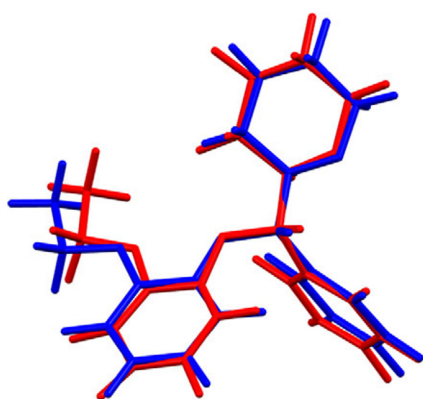

Figure 5. Comparison of the refined structure of reboxetine cation 1 (red) to the VASP-optimized structure (blue). The comparison was generated using the Mercury Calculate/Molecule Overlay tool; the rms difference is 0.323 Å. Image generated using Mercury (Macrae et al., 2020).
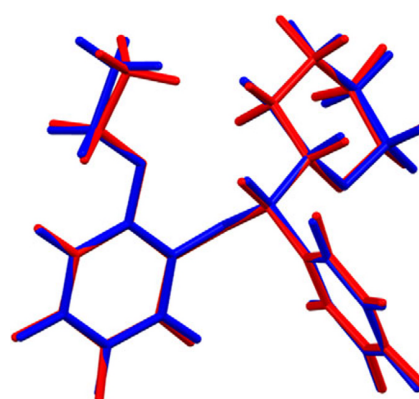

Figure 6. Comparison of the refined structure of reboxetine cation 2 (red) to the VASP-optimized structure (blue). The comparison was generated using the Mercury Calculate/Molecule Overlay tool; the rms difference is 0.120 Å. Image generated using Mercury (Macrae et al., 2020).

cation 2, calculated using the Mercury Calculate/Molecule Overlay tool, are 0.323 and 0.120 Å (Figures 5 and 6). The largest differences are 0.873 Å at C34 and 0.299 Å at C81 in the side chains. The agreements are within the normal range for correct structures (van de Streek and Neumann, 2014). The asymmetric unit is illustrated in Figure 7. The remaining discussion will emphasize the VASP-optimized structure.

All of the bond distances and bond angles, and most of the torsion angles, fall within the normal ranges indicated by a Mercury Mogul Geometry check (Macrae et al., 2020). The O1–C46–C44–O3 torsion angle lies on the tail of the *trans* portion of a *trans/gauche* distribution. The C93–O48–C68–

C76 torsion angle lies on a long tail of a distribution of similar torsion angles. Thus, both cations are slightly unusual.

The two independent cations have similar overall shapes (Figure 8). The rms displacement is 0.446 Å. The main difference is in the conformation of the center of the cations, at O1/C46 and O48/C93. Quantum chemical geometry optimization of isolated reboxetine cations (DFT/B3LYP/6-31G*/water) using Spartan '24 (Wavefunction, 2023) indicated that both cations are very close to local minima and that cation 1 is 0.8 kcal/mol lower in energy than cation 2. This difference is less than the expected uncertainty of such calculations; hence, the two conformations should be considered equivalent in
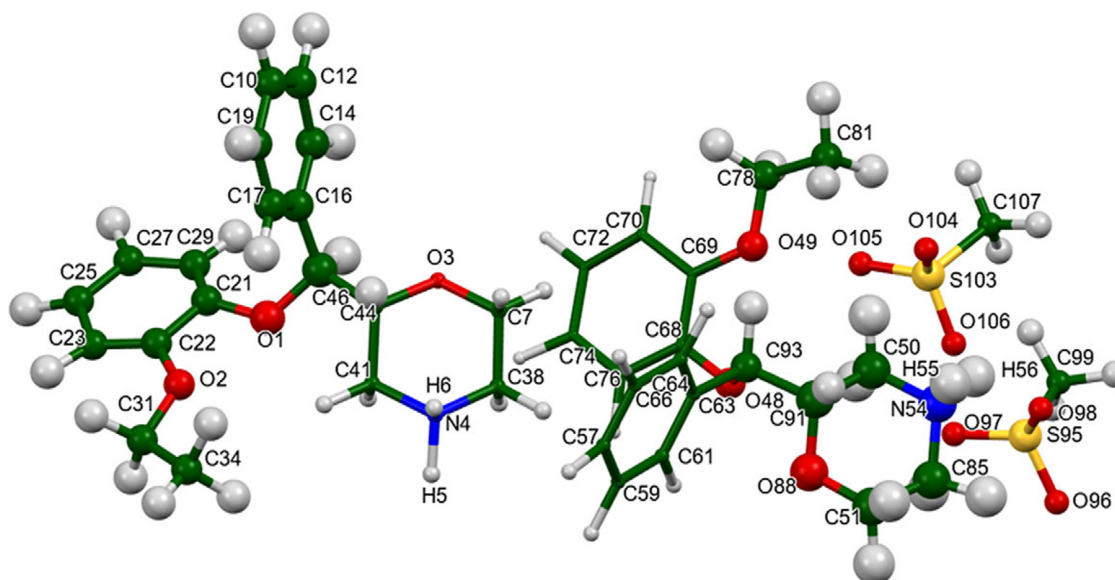
Figure 7. The asymmetric unit of reboxetine mesylate Form 2, with the atom numbering. The atoms are represented by 50% probability spheroids. Image generated using Mercury (Macrae et al., 2020).
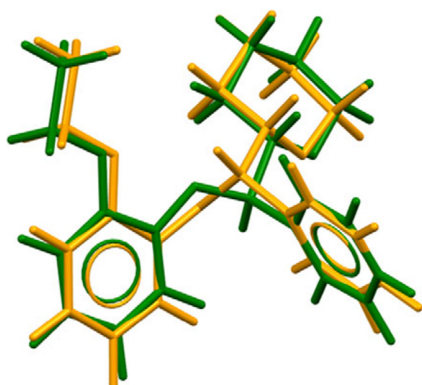

Figure 8. Comparison of cation 1 (green) and cation 2 (orange) in reboxetine mesylate Form 2. The rms difference is 0.446 Å. Image generated using Mercury (Macrae et al., 2020).

energy. The global minimum-energy conformation is 7.4 kcal/mol lower in energy than cation 1, and has a different orientation of the morpholine ring (rotated ~60°).

The crystal structure (Figure 9) consists of double columns of anions and cations along the *a*-axis, columns that are clearer when the figure is manipulated in real time. Hydrogen bonds (discussed below) link the cations and the anions along this axis. The mean plane of the C10–C19 phenyl ring in cation 1 is approximately (0, −1, 2) and the C21–C29 phenyl ring is approximately (3, 1, −1). The comparable planes for cation 2 are approximately (0, 1, 4) and (−3, 1, 1). The Mercury Aromatics Analyser indicates a strong interaction (distance = 5.04 Å) between phenyl rings of cations 1 and 2, a moderate interaction (distance = 6.35 Å) between phenyl rings, and weak interactions (distances > 8.0 Å).

Analysis of the contributions to the total crystal energy of the structure using the Forcite module of Materials Studio (Dassault Systèmes, 2024) indicates that angle distortion terms dominate the intramolecular energy. The intermolecular energy is dominated by van der Waals attractions and electrostatic repulsions, which, in this force field-based analysis,

also include hydrogen bonds. The hydrogen bonds are better discussed using the results of the DFT calculation.

As expected, each protonated N in the morpholine rings acts as a donor in a strong N–H⋯O hydrogen bond to an anion (Table III). The energies of the N–H⋯O hydrogen bonds were calculated using the correlation of Wheatley and Kaduk (2019). These hydrogen bonds link the cations and the anions into zig-zag chains along the *a*-axis (Figure 10). There are many C–H⋯O hydrogen bonds between the cations and the anions, and also two C–H⋯O hydrogen bonds between the cations.

In Form 1, the protonated N in the morpholine ring also acts as a donor in two strong N–H⋯O hydrogen bonds to an anion (Table IV). In this form, two cations and two anions form a ring, with a graph set *R4,4(12)* (Etter, 1990; Bernstein et al., 1995; Motherwell et al., 2000) (Figure 11). Several C–H⋯O hydrogen bonds, as well as cation–anion, anion–cation, and cation–cation interactions, also contribute to the lattice energy.

The volume enclosed by the Hirshfeld surface of reboxetine mesylate Form 2 (Figure 12; Hirshfeld, 1977; Spackman et al., 2021) is 980.45 $Å^3$, 98.67% of one-fourth of the unit cell volume. The packing density is thus typical. The only significant close contacts (red in Figure 12) involve the hydrogen bonds. The volume/non-hydrogen atom is typical at 17.7 $Å^3$.

The Bravais–Friedel–Donnay–Harker (Bravais, 1866; Friedel, 1907; Donnay and Harker, 1937) algorithm suggests that we might expect isotropic morphology for reboxetine mesylate. A second-order spherical harmonic model was included in the refinement. The texture index was 1.020(0), indicating that the preferred orientation was slight in this rotated capillary specimen.

DEPOSITED DATA

The powder pattern of reboxetine mesylate from this synchrotron dataset has been submitted to the International Centre for Diffraction Data (ICDD) for inclusion in the
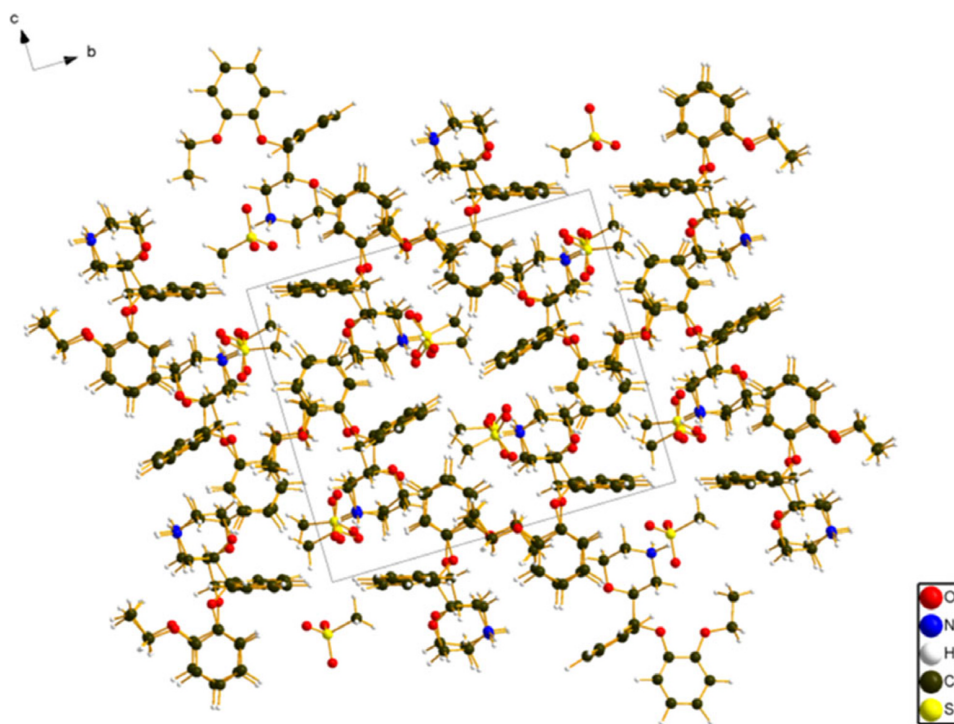
Figure 9. The crystal structure of reboxetine mesylate Form 2, viewed down the *a*-axis. Image generated using Diamond (Crystal Impact, 2023).

TABLE III. Hydrogen bonds (CRYSTAL23) in reboxetine mesylate Form 2

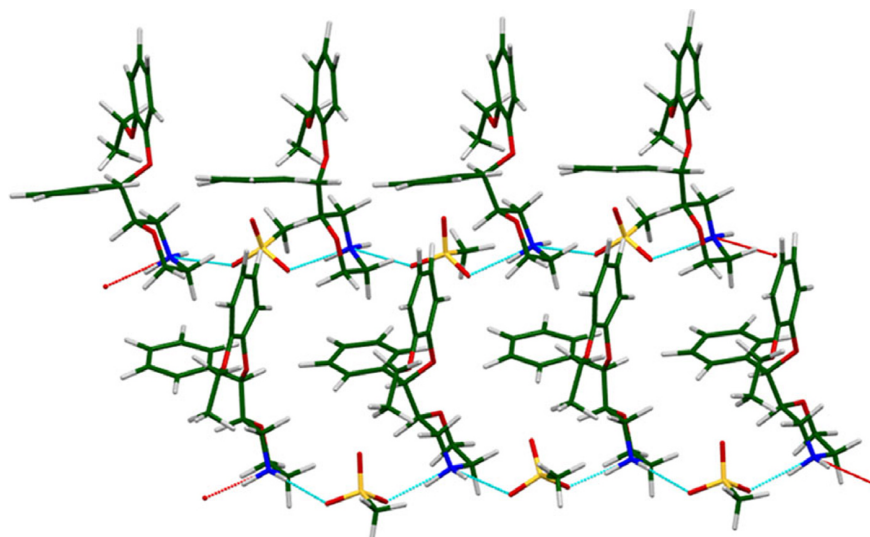| H bond	D–H, Å	H···A, Å	D···A, Å	D–H···Å, °	Mulliken overlap, *e*	*E*, kcal/mol
N4–H5···O104	1.058	1.718	2.736	160.0	0.078	6.4
N4–H6···O96	1.058	1.793	2.848	174.0	0.080	6.5
N54–H55···O106	1.053	1.838	2.853	160.6	0.070	6.1
N54–H56···O98	1.054	1.819	2.814	155.9	0.070	6.1
C17–H18···O97	1.92	2.437	3.444	152.8	0.02	
C19–H20···O88	1.091	2.607	3.561	145.7	0.015	
C19–H20···O48	1.091	2.568	3.533	146.9	0.013	
C23–H24···O97	1.089	2.594	3.566	148.1	0.014	
C70–H71···O105	1.089	2.437	3.402	147.0	0.017	
C76–H77···O106	1.092	2.608	3.608	152.0	0.017	
C85–H87···O97	1.097	2.740	3.631	138.1	0.011	
C91–H92···O106	1.106	2.638	3.452	129.8	0.010	
C31–H32···O48	1.102	2.587	3.536	143.7	0.012	
C93–H94···O49	1.101	2.334	2.996	116.8	0.012	

Figure 10. The hydrogen-bonded chains in reboxetine mesylate Form 2. The *a*-axis is horizontal. Image generated using Mercury (Macrae et al., 2020).

TABLE IV. Hydrogen bonds (CRYSTAL23) in reboxetine mesylate Form 1

| H bond	D–H, Å	H···A, Å	D···A, Å	D–H···A, °	Mulliken overlap, e	E, kcal/mol
N9–H54···O6	1.052	1.728	2.719	155.3	0.067	6.0
N9–H55···O4	1.048	1.786	2.765	153.8	0.065	5.9
C14–H15···O45	1.092	2.230	3.312	171.2	0.024	
C17–H18···O2	1.087	2.421[a]	2.792	98.6	0.010	
C31–H32···O6	1.102	2.289	3.294	150.8	0.018	
C34–H36···O2	1.095	2.526	3.574	159.8	0.013	
C42–H33···O4	1.095	2.460	3.552	174.8	0.019	
C7–H50···O2	1.097	2.346[a]	2.724	97.9	0.011	
C7–H51···O5	1.096	2.464	3.197	123.1	0.012	
C38–H40···O4	1.093	2.361	3.360	151.2	0.021	

[a]Intramolecular.
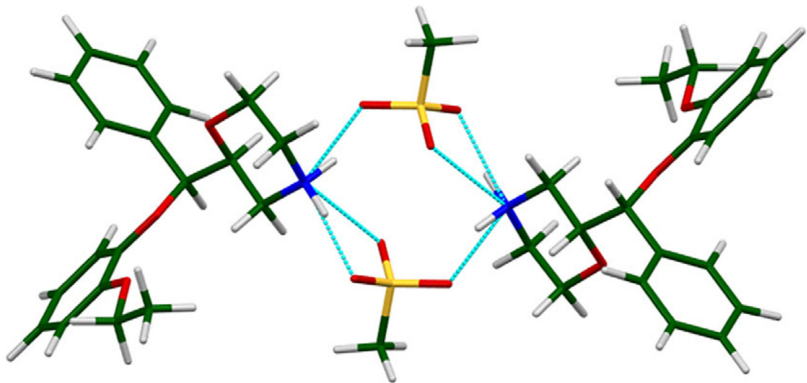
Figure 11. The hydrogen-bonded rings in reboxetine mesylate Form 1. Image generated using Mercury (Macrae et al., 2020).
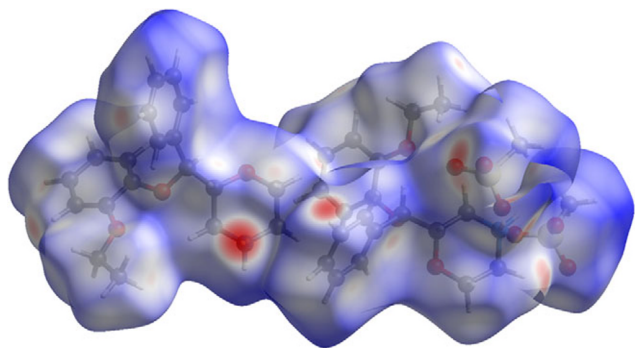

Figure 12. The Hirshfeld surface of reboxetine mesylate Form 2. The intermolecular contacts longer than the sum of the van der Waals radii are colored blue, and the contacts shorter than the sum of the radii are colored red. The contacts equal to the sum of radii are white. Image generated using CrystalExplorer (Spackman et al., 2021).

Powder Diffraction File. The Crystallographic Information Framework (CIF) files containing the results of the Rietveld refinement (including the raw data) and the DFT geometry optimization were deposited with the ICDD. The data can be requested at pdj@icdd.com.

ACKNOWLEDGEMENTS

FUNDING STATEMENT

COMPETING INTEREST

The authors have no competing interests to declare.

REFERENCES

Altomare, A., C. Cuocci, C. Giacovazzo, A. Moliterni, R. Rizzi, N. Corriero, and A. Falcicchio. 2013. "EXPO2013: A Kit of Tools for Phasing Crystal Structures from Powder Data." *Journal of Applied Crystallography* 46: 1231–35.

Bernstein, J., R. E. Davis, L. Shimoni, and N. L. Chang. 1995. "Patterns in Hydrogen Bonding: Functionality and Graph Set Analysis in Crystals." *Angewandte Chemie International Edition in English* 34: 1555–73.

Bravais, A. 1866. *Etudes Cristallographiques*. Paris: Gauthier Villars.

Bruno, I. J., J. C. Cole, M. Kessler, J. Luo, W. D. S. Motherwell, L. H. Purkis, B. R. Smith, et al. 2004. "Retrieval of Crystallographically Derived

Molecular Geometry Information." *Journal of Chemical Information and Computer Sciences* 44: 2133–44.

Crystal Impact. 2023. *Diamond V. 5.0.0.* Bonn: Crystal Impact – Dr. H. Putz & Dr. K. Brandenburg.

Dassault Systèmes. 2024. *BIOVIA Materials Studio 2025.* San Diego, CA: BIOVIA.

Donnay, J. D. H., and D. Harker. 1937. "A New Law of Crystal Morphology Extending the Law of Bravais." *American Mineralogist* 22: 446–67.

Erba, A., J. K. Desmarais, S. Casassa, B. Civalleri, L. Donà, I. J. Bush, B. Searle, et al. 2023. "CRYSTAL23: A Program for Computational Solid State Physics and Chemistry." *Journal of Chemical Theory and Computation* 19: 6891–932. https://doi.org/10.1021/acs.jctc.2c00958.

Etter, M. C. 1990. "Encoding and Decoding Hydrogen-Bond Patterns of Organic Compounds." *Accounts of Chemical Research* 23: 120–26.

Friedel, G. 1907. "Etudes sur la loi de Bravais." *Bulletin de la Société Française de Minéralogie* 30: 326–455.

Gatti, C., V. R. Saunders, and C. Roetti. 1994. "Crystal-Field Effects on the Topological Properties of the Electron-Density in Molecular Crystals – the Case of Urea." *Journal of Chemical Physics* 101: 10686–96.

Hirshfeld, F. L. 1977. "Bonded-Atom Fragments for Describing Molecular Charge Densities." *Theoretica Chemica Acta* 44: 129–38.

Kabekkodu, S., A. Dosen, and T. N. Blanton. 2024. "PDF-5+: A Comprehensive Powder Diffraction File™ for Materials Characterization." *Powder Diffraction* 39: 47–59.

Kaduk, J. A., C. E. Crowder, K. Zhong, T. G. Fawcett, and M. R. Suchomel. 2014. "Crystal Structure of Atomoxetine Hydrochloride (Strattera), $C_{17}H_{22}NOCl$." *Powder Diffraction* 29: 269–73.

Kalofonos, I., G. P. Stahly, W. Martin-Doyle, W. Lai, D. T. Jonaitis, and A. G. Lityo. 2010. "Novel Forms of Reboxetine." U.S. Patent Application US 2010/0069389 A1.

Kresse, G., and J. Furthmüller. 1996. "Efficiency of Ab-Initio Total Energy Calculations for Metals and Semiconductors Using a Plane-Wave Basis Set." *Computational Materials Science* 6: 15–50.

Leontowich, A. F. G., A. Gomez, B. Diaz Moreno, D. Muir, D. Spasyuk, G. King, J. W. Reid, C.-Y. Kim, and S. Kycia. 2021. "The Lower Energy Diffraction and Scattering Side-Bounce Beamline for Materials Science at the Canadian Light Source." *Journal of Synchrotron Radiation* 28: 961–69.

Lin, J., G. Bu, J. Unge, and T. Gonen. 2024. "Uncovering the Elusive Structures and Mechanisms of Prevalent Antidepressants." BioRchiv Preprint. https://doi.org/10.1101/2024.01.04.574264.

Macrae, C. F., I. Sovago, S. J. Cottrell, P. T. A. Galek, P. McCabe, E. Pidcock, M. Platings, et al. 2020. "*Mercury 4.0*: From Visualization to Design and Prediction." *Journal of Applied Crystallography* 53: 226–35.

Materials Design, Inc. 2024. *MedeA 3.7.2.* San Diego, CA: Materials Design Inc.

Motherwell, W. D. S., G. P. Shields, and F. H. Allen. 2000. "Graph-Set and Packing Analysis of Hydrogen-Bonded Networks in Polyamide Structures in the Cambridge Structural Database." *Acta Crystallographica B* 56: 857–71.

Peintinger, M. F., D. Vilela Oliveira, and T. Bredow. 2013. "Consistent Gaussian Basis Sets of Triple-Zeta Valence with Polarization Quality for Solid-State Calculations." *Journal of Computational Chemistry* 34: 451–59.

Spackman, P. R., M. J. Turner, J. J. McKinnon, S. K. Wolff, D. J. Grimwood, D. Jayatilaka, and M. A. Spackman. 2021. "CrystalExplorer: A Program for Hirshfeld Surface Analysis, Visualization and Quantitative Analysis of Molecular Crystals." *Journal of Applied Crystallography* 54: 1006–11. https://doi.org/10.1107/S1600576721002910; https://crystalexplorer.net.

Stephens, P. W. 1999. "Phenomenological Model of Anisotropic Peak Broadening in Powder Diffraction." *Journal of Applied Crystallography* 32: 281–89.

Sykes, R. A., P. McCabe, F. H. Allen, G. M. Battle, I. J. Bruno, and P. A. Wood. 2011. "New Software for Statistical Analysis of Cambridge Structural Database Data." *Journal of Applied Crystallography* 44: 882–86.

Toby, B. H., and R. B. Von Dreele. 2013. "GSAS II: The Genesis of a Modern Open Source All Purpose Crystallography Software Package." *Journal of Applied Crystallography* 46: 544–49.

van de Streek, J., and M. A. Neumann. 2014. "Validation of Molecular Crystal Structures from Powder Diffraction Data with Dispersion-Corrected Density Functional Theory (DFT-D)." *Acta Crystallographica Section B: Structural Science, Crystal Engineering and Materials* 70: 1020–32.

Wavefunction, Inc. 2023. *Spartan '24. V. 1.0.0.* Irvine, CA: Wavefunction, Inc.

Wheatley, A. M., and J. A. Kaduk. 2019. "Crystal Structures of Ammonium Citrates." *Powder Diffraction* 34: 35–43.

Zampieri, M., A. Airoldi, and A. Martini. 2003. "Pharmaceutical Salts of Reboxetine." European Patent Application EP 1515959 A1.